Study of Mechanical Properties of Carbon Steel Plate SA-516 Gr. 70 Welded by SAW Using Square-Shape Joint Design

Mohannad Yousif Hanna **Samir Ali Amin** **Abdulaziz Saud Khider**

Mechanical Engineering Department, University of Technology, Baghdad-Iraq

mohannad_hanna@yahoo.com alrabiee2002@yahoo.com abdulaziz.saud87@gmail.com

Submission date:- 3/7/2019	Acceptance date:- 29/8/2019	Publication date:-26/9/2019

Abstract:

Submerged arc welding (SAW) is a fusion type welding and it is considered as one of the most important welding types due to its inherent capabilities of high welding speed, high deposition rate, welding large thickness plates owing to its deep penetration characteristic and many other advantages. In this study, the goal was to investigate the effect of welding parameters, namely (welding current and welding speed) as well as the joint design on the mechanical properties (yield stress, bending force on the face of the weldment and hardness of the weld metal. Experiments were conducted employing Design of Experiment (DOE) software and Response Surface Methodology (RSM) technique. The experiments were performed by welding (26) pieces of ASME SA-516 Gr. 70 steel plate with dimensions of (300 mm × 150 mm × 10 mm) to produce (13) specimens depending upon the design matrix developed via the DOE. Results manifested that the optimum process parameters for maximum yield stress, maximum bending force and minimum hardness were (202.659 MPa, 21.662 KN and 139.232 HV), respectively at (425 amps) welding current and (35 cm/min) welding speed, where the arc voltage was held constant at (37 volts). Finally, it was found that the predicted and experimental results of yield stress, bending force and hardness agree very well according to the ultimate error (1.5%, 1.3%, and 3.4 %), respectively.

Keywords: Welding parameters, SAW, Mechanical Properties, DOE, RSM.

1. Introduction

A large number of works has been done by many researchers in the field of submerged arc welding. This paper briefly covers the previously published works carried out by researchers in the various fields concerning with the experimental investigation, modeling and optimization of SAW process parameters that have effect on the mechanical properties. In general, the tensile strength properties and hardness of the welded joints increase with the increase in number of passes and in the contrary, the ductility and toughness decrease gradually. These changes in mechanical behavior can be related to the observed microstructural properties, particularly the amount of morphology and the ferrite delta distribution [1]. The deposition rate increases greatly with the increase in welding speed at all values of heat inputs investigated, without affecting the weldment soundness. Hardness values decrease with an increase in welding speed and heat input [2]. With the formation of acicular ferrite, the ultimate tensile strength and yield strength of weld metal increases for fluxes containing TiO2, the inclusion percentage of welds reduces the area of reduction and elongation percentages [3]. It was deduced that the weld metal grain structure and heat affected zone are affected by the heat input. Both the ultimate tensile strength and yield strength decreased with the increase in heat input, while the percentage of elongation has increased [4]. The testing results showed the significance of cladding methods and estimated heat treatment influences on the stated mechanical properties. The microhardness increased with the decrease in heat input, also it was found that the percentage of graphite and slow cooling rate which resulted in better mechanical properties [5]. It was obtained that the high cooling rate and low heat input caused the higher hardness [6].

The results depicted that the current had a significant effect on the hardness, where with the increase of welding current from 300 A to 330 A, the hardness decreased [7]. The speed of welding and the arc voltage possess an important influence upon the residual stress. The speed of welding mostly

raised the residual stresses over the entire chosen levels of input [8]. The results revealed that the microhardness decrease significantly with the increase in welding current [9].

From the previous work it can be concluded that a lot of works were done for the optimization of mechanical properties, where they have taken the effect of number of passes of welding, type/amount of inclusions and the evolution of weld microstructure, influence of flux chemical composition, addition of alloying element powder (nickel and molybdenum), TiO_2 addition to the flux composition and many other effects. But, there is a little work that considered the modeling and optimization the effect of welding parameters in SAW pressure vessel materials on their mechanical properties, experimentally and theoretically. Accordingly, the objective of the present paper is first to study the effect of using the submerged arc welding parameters, including current, welding speed with the use of square-shape joint design on the mechanical properties of low carbon steel plate SA-516 Gr. 70 that is usually utilized for manufacturing pressure vessels. Design of Experiment (DOE) method will be used to model and optimize the input welding parameters (welding current and welding speed) together with the outputs, including yield stress, maximum bending force and hardness of the SAW specimens for comparing the predicted results with the experimental ones.

2. Experimental Work

2.1 Used Material

The base material used in the welding process was low carbon steel plate **(ASME SA-516 Gr. 70)** with a thickness of 10 mm; it is usually employed for producing tanks in the petroleum industry, boilers, and pressure vessels. All plates were submerged welded utilizing ASME SFA-5.17M EM12K wire (3.25 mm diameter) and ASME SFA-5.17M F48A2 flux having 0.8 basicity index. Table (1) lists the chemical analyses of the used and nominal ASME SA-516 Gr. 70 for a plate thickness of less than (12.5 mm), and Table (2) depicts their mechanical properties for the purposes of comparison and conformity. Also, the chemical composition of the used and nominal of ASME SFA-5.17M EM12K is given in Table (3).

Table (1): Chemical compositions of nominal and used steel plate (ASME SA-516 Gr. 70) [10]**.**

Material wt.%	%C Max	%Mn	%Si	%P Max	%S Max
Nominal (for t ≤ 12.5 mm)	0.27	0.79/1.3	0.13/0.45	0.035	0.035
Used	0.22	1.31	0.3	---	---

Table (2): Mechanical properties of nominal and used steel plate (ASME SA-516 Gr. 70) [10]**.**

	Tensile strength Mpa	Yield strength Mpa	Elongation (%)	Bending force KN	Hardness HV
Nominal	485/620	260 (min)	21 (min)	---	---
Used	520	385	35	36	160

2.2 Submerged Arc Welding Conditions

To investigate the influence of the input factors on the hardness and mechanical properties developed via the process of SAW, two welding factors (current and travel speed) were utilized as an individual factor with five levels as shown in the Table (4). These levels were chosen depending upon the actual practices that used in the Heavy Engineering Equipment State Company (HEESCo).

Table (3): Chemical composition of nominal and used electrode wire (Askanyak AS S2Si).

	Materials wt. %					
	%C	%Mn	%Si	%P	%S	%Cu
Nominal [11]	0.05/0.15	0.8/1.25	0.1/0.35	0.03 (max)	0.03 (max)	0.35 (max)
Used [12]	0.07	1.0	0.15	---	0.025	---

Table (4): Used levels of input factors

Input parameter	Levels				
	-2	-1	0	+1	+2
Welding current (Ampere)	275	325	375	425	475
Welding speed (cm/min)	20	25	30	35	40

2.3 Welding Procedure

First, the plate was cut to (26) pieces having dimensions (300x150x10 mm) and their surfaces were then cleaned for the oxides and contamination removal via the sand blasting. Milling cutter was utilized to produce a square joint in a single-butt weld joint that then submerged arc welded to make (13) specimens. All the experiments were achieved depending upon design matrix (Table 5) made via the DOE software with five levels of input factors for finding out their effect on the mechanical properties induced in the SAW process. Fig. (1) Shows a simple schematic of the type of joint design used in the experiment. Fig. (2) Displays the used welding machine, type (EsabA2 Multitrack with the A2-A6 process controller PEK).

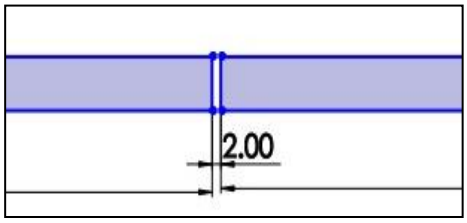

Fig. (1): A simple schematic of joint design used in the experiment

Fig. (2): EsabA2 Multitrack with the A2-A6 process controller PEK

Table (5): Experimental design matrix for both actual input factors and responses

Std. No.	Welding current (Ampere)	Welding speed (cm/min)	Yield stress (MPa)	Maximum bending force-face	Hardness (HV)
1	325	25	152.74	21.58	203.25
2	425	25	183.34	25.83	195.30
3	325	35	170.84	19.63	185.3
4	425	35	205.66	21.95	134.65
5	275	30	166.35	19.19	206.41
6	475	30	222.67	24.84	164.93
7	375	20	153.51	27.46	214.13
8	375	40	196.34	20.21	146.67
9	375	30	169.74	20.76	173.48
10	375	30	167.59	20.47	175.69
11	375	30	170.23	19.85	177.74
12	375	30	171.84	20.59	179.28
13	375	30	166.42	20.66	174.55

2.4 Measurements of Yield Stress, Maximum Bending Force and Hardness

All the tensile and bending tests were conducted in the Department of Production Engineering and Metallurgy at the University of Technology using WDW-200E Testing machine with a constant load of (0.04 KN), crosshead speed of (2 mm/min). The average of yield stress and max bending force was taken from two tests, as listed in Table (5). Hardness measurements were carried out at the Department of Mechanical Engineering at the University of Technology using LARYEE HBRVS testing machine on a polished surface specimen at the neutral axis of the weld metal only, taking the mean of three readings. The indents were formed by a diamond indenter, in the form of a right pyramid with a square base and an angle of 136 degrees between opposite faces subjected to a load of 100 kgf (980.7 N), and the resident time was 10 seconds. The indentation imprinted on the specimen by the indenter was measured and recorded, as given in Table (5).

2.5 Design of Experiments

In the current investigation, the RSM approach was employed for developing mathematical model depending upon the experimental results. Quadratic functions of the response surface must be regarded, since the curvature may be insufficiently modeled via employing the first-order function during the ranges of the common working states. 13 experiments were conducted depending upon the experimental design matrix. The tests were carried out randomly at various coded levels from (-2) to (+2) utilized with each factor, where each used level corresponded to an actual value adapted to the coded one. Therefore, the welding input factors investigated include the current and the travel speed. The experimental design matrix employed for the input factors with the resulted output (response) values is elucidated in the Table (5). The prediction model with a 95% confidence level was established via "DESIGN EXPERT Version 10."

3. Results and Discussion

3.1 Modeling of Yield Stress

The proper model was first chosen and made via employing the approach of RSM, and then the characteristics of the response were utilized to determine the regression expressions to the model. The experimental results given in Table (5) were employed to make the regression expressions, which were drawn to explore the process factors effect on the various characteristics of response. Analysis of variance (ANOVA) for the response surface quadratic model for yield stress was achieved with backwards elimination of insignificant coefficients for analyzing statistically the results, as given in the Table (6).

The F-value of (233.92) of the model shown in the Table (6) depicts that the model is 'significant' with 95% confidence level. The "Prob> F" values less than (0.05) indicate that the terms of this model are important. In such case, the terms (A, B, A^2 and B^2) are significant ones in such model. Thus, such model explains that the current (A) of welding, speed (B) of welding and their squared terms possess the largest impact on the yield stress. Also, the lack of fitting refers to a good model.

The tentative quadratic predicted model established for yield stress induced in the SAW of (ASME SA-516 Gr. 70) low carbon steel is given as follows:

Yield stress = + 405.36121 - 1.61041* Current - 1.40510* Welding speed + 2.54291E-003* Current^2 + 0.058441Welding speed^2 ---------- (1)

Table (6): ANOVA for response surface quadratic model for yield stress

Source	Sum of Squares	df	Mean Square	F Value	P-value Prob > F
Model	4895.79	4	1223.95	233.92	< 0.0001 **significant**
A-Current	37.64	1	37.64	7.19	0.0278
B-Welding speed	1324.68	1	1324.68	253.17	< 0.0001
A^2	926.05	1	926.05	176.99	< 0.0001
B^2	48.91	1	48.91	9.35	0.0156
Residual	41.86	8	5.23		
Lack of Fit	23.22	4	5.81	1.26	0.4182 **not significant**
Pure Error	18.64	4	4.66		
Cor Total	4937.65	12			
Std. Dev.	2.29		**R-Squared**	0.9915	
Mean	176.71		**Adj. R-Squared**	0.9873	
C.V. %	1.29		**Pred. R-Squared**	0.9624	
PRESS	185.44		**Adeq. Precision**	51.220	

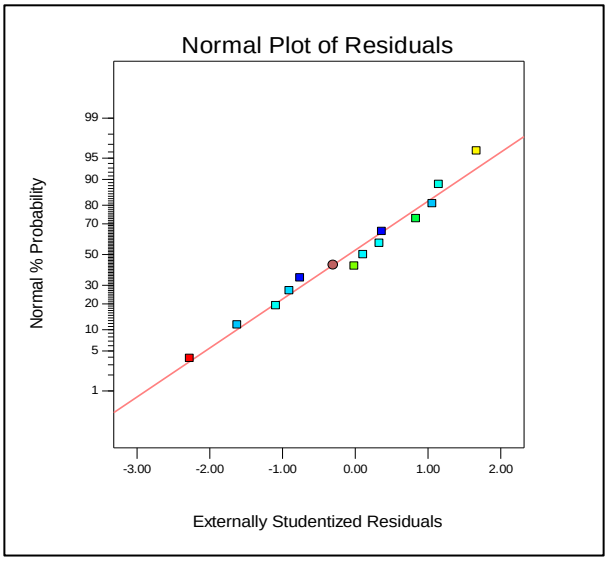

Fig. (3): Normal distribution of yield stress data

The model adequacy checking was performed via the analysis of residual, and the outputs are evinced in the Figures (3 and 4), respectively. The plot of normal probability is presented in Fig. (3). The errors are distributes normally as appeared in such figure, where the residuals exist on a straight line. The standardized residuals relevant to the predicted results are shown in the Fig. (4).

The residuals don't appear any explicit unfamiliar style and are distributed in both positive and negative direction. This demonstrates the adequacy of the model. Fig. (5) illustrates that the yield stress predicted results are close to the actual ones that measured in tests, explaining that both predicted and experimental outputs possess a good agreement. This output is confirmed via the (2D) contour graph and (3D) surface graph displayed in Figures (6 and 7), respectively in terms of current and travel speed of welding.

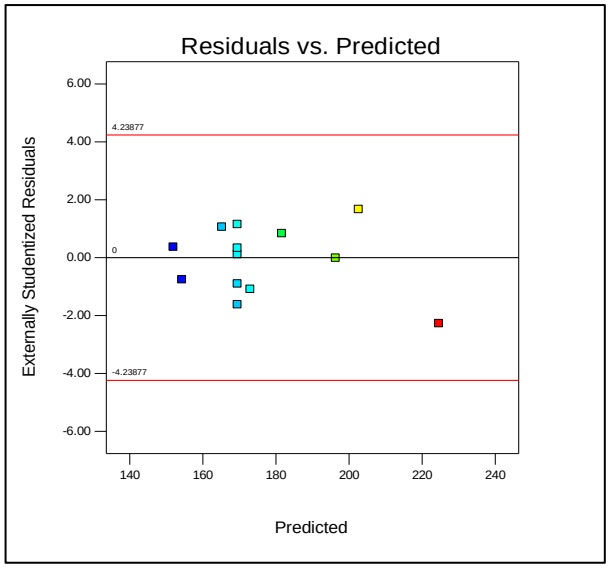

Fig. (4): Residual versus predicted data

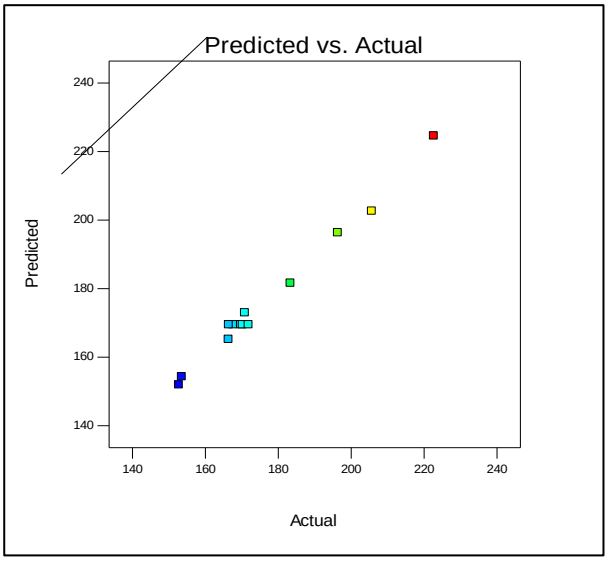

Fig. (5): Predicted versus actual data

It can be seen from Fig. (6) that increasing the welding speed caused increasing yield stress and increasing current also resulted in an increase in yield stress. This is confirmed by Fig. (7) showing that the maximum yield stress occurred at the highest level of welding speed (35 cm/min) and the highest level of current (425 Ampere). This result is likely attributed to the effect that increasing the welding speed at higher current resulted less thermal effect on the material, higher cooling rate and deposition rate, thus increasing the yield stress.

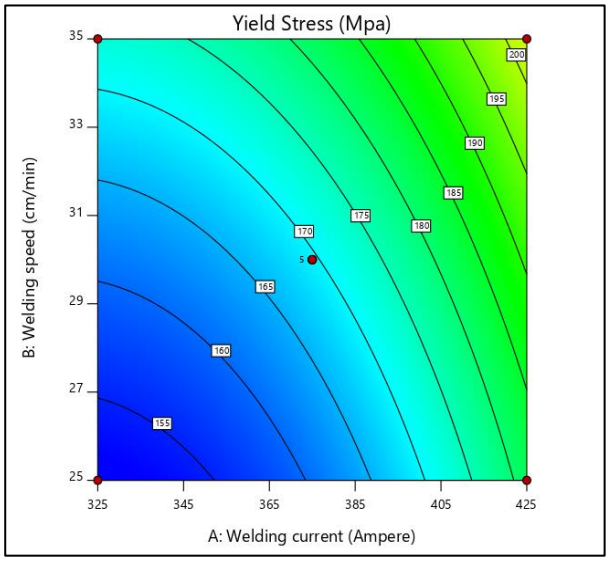

Fig. (6): 2D contour graph of yield stress as a function of welding speed and welding current

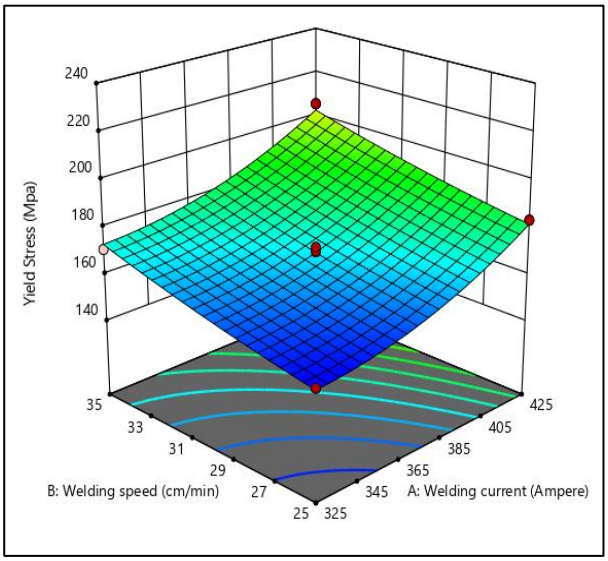

Fig. (7): 3D surface plot of yield stress as a function of welding speed and welding current

3.2 Modeling of Maximum Bending Force

In a similar way, for the maximum bending force for the face of the weld results given in Table (5), a quadratic model in the coded terms was analyzed using the backwards elimination of the unimportant coefficients. Table (7) reveals the statistical analysis of variance (ANOVA), and this model is significant at 95% confidence. In such model, the welding speed (B) and the squared terms (A^2) and (B^2) are all significant. This model explains that these three terms possess the greatest impact on the maximum bending force. Also, there is no interaction between the current and welding speed. Also, the lack of fitting test refers to a good model.

The final equation of maximum bending force (face) in terms of the actual factors is:

Maximum bending force = +72.59630 - 0.089247* Current - 2.38307* Welding speed +1.58707E-004* Current^2 + 0.034071* Welding speed^2 ----------(2)

Table (7): ANOVA for response surface quadratic model for maximum bending force (Face)

Source	Sum of Squares	df	Mean Square	F Value	P-value Prob > F
Model	78.28	4	19.57	56.56	< 0.0001 **significant**
A-Current	0.19	1	0.19	0.54	0.4825
B-Welding speed	34.44	1	34.44	99.55	< 0.0001
A^2	3.61	1	3.61	10.43	0.0121
B^2	16.62	1	16.62	48.05	0.0001
Residual	2.77	8	0.35		
Lack of Fit	2.25	4	0.56	4.33	0.0923 **not significant**
Pure Error	0.52	4	0.13		
Cor Total	81.04	12			
Std. Dev.	0.59		**R-Squared**	0.9658	
Mean	21.77		**Adj. R-Squared**	0.9488	
C.V. %	2.70		**Pred. R-Squared**	0.8638	
PRESS	11.04		**Adeq. Precision**	23.932	

For checking statistically, the adequacy of this model, the plot of the normal probability of residuals (Fig. 8) for the max bending force results showed that generally the residuals (errors) fall on a straight line and they are distributed normally. Also, there are no clear patterns or uncommon structure, implying accurate models. The standardized residuals relevant to the predicted results are shown in the Fig. (9). The residuals do not appear any explicit uncommon style and are distributed in both positive and negative direction. This clarifies the adequacy of the model. Fig. (10) shows the predicted versus the actual data for comparison purpose.

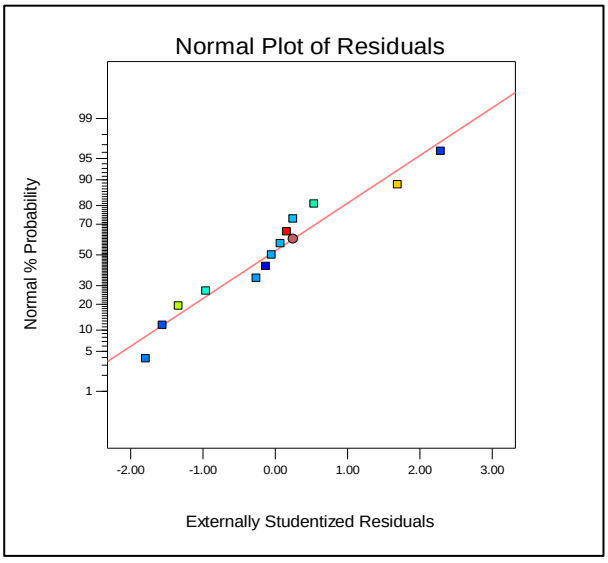

Fig. (8): Normal distribution of maximum bending force data

Referring to the Fig. (11) for the (2D) contour plot, one can note that, generally, the maximum bending force has the highest value at a higher level of welding current and lower value of welding speed due to high deposition rate on the face of the weld. It can also be seen that at the higher current and higher welding speed, the bending force decreases. Where, Fig. (12) manifests the (3D) plot of bending force in terms of welding current and travel speed and confirms that the increment of arc current remained the maximum bending force constant at a lower level of welding speed, while the increase of welding speed decreases the maximum bending force at lower and higher level of welding current. However, the welding current alone is not influential during welding over the used range of its levels.

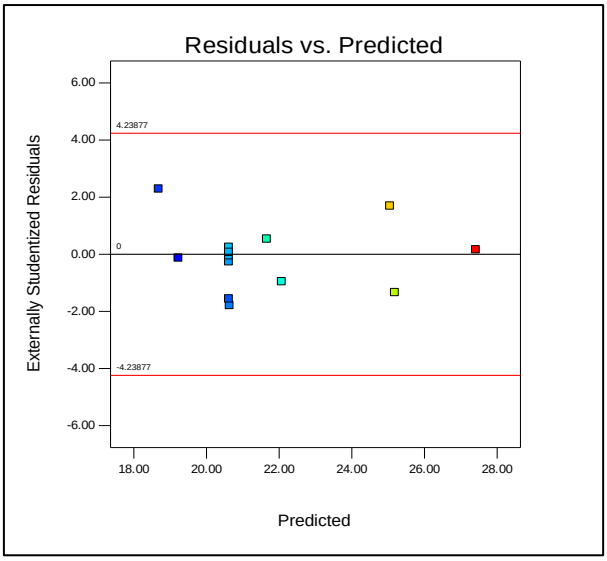

Fig. (9): Residual versus predicted data

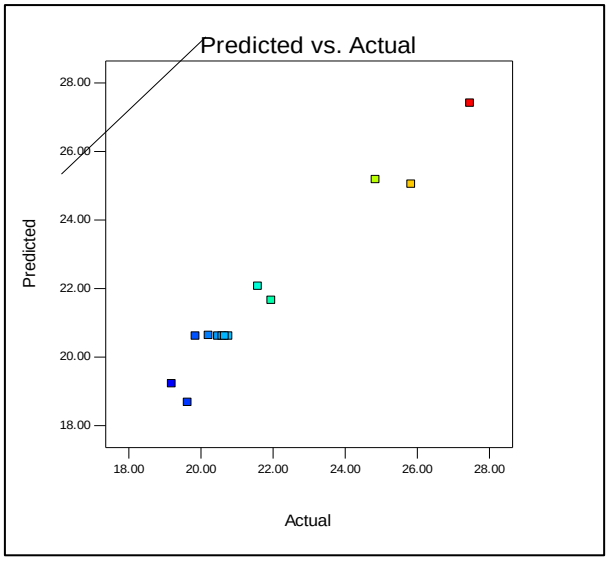

Fig. (10): Predicted versus actual data

3.3 Modeling of Hardness

The average responses obtained for hardness were utilized in the calculation of the models of response surface per response employing the method of the least squares. For the hardness prediction, a quadratic model in the coded terms was analyzed via the backwards elimination of unimportant coefficients.

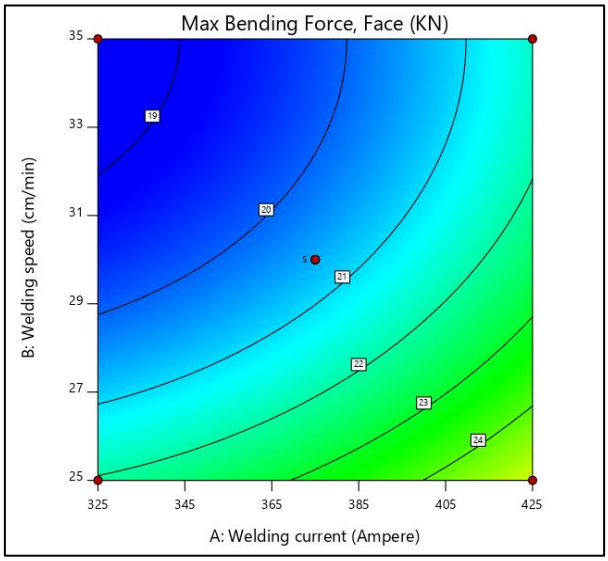

Fig. (11): 2D contour graph of maximum bending force as a function of welding speed and welding current

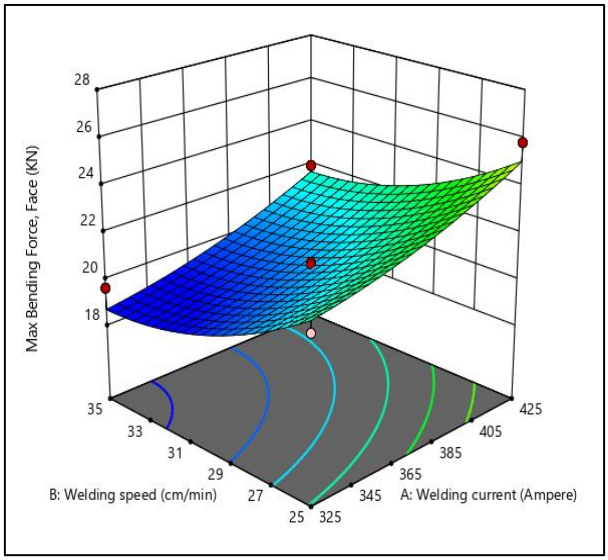

Fig. (12): 3D surface plot of maximum bending force as a function of welding speed and welding current

This model reveals that the terms (A), the interaction (AB) and (A2) are significant. This means that these three terms (welding current, its squared term and the interaction of both current and welding speed) have the highest impact on hardness. Table (8) manifests the statistical analysis of variance (ANOVA) produced by the software for the rest of terms. This model is significant with 95% confidence level. The lack of fitting test indicates a good model.

The final equation of harness in terms of the actual factors is:

Hardness = + 9.22569 + 0.42134* Current +12.45383* Welding speed - 0.042700 * Current * Welding speed + 8.31630E-004 * Current^2 ----------(3)

Table (8): ANOVA for response surface quadratic model for hardness

Source	Sum of Squares	df	Mean Square	F Value	P-value Prob > F
Model	6032.72	4	1508.18	102.53	< 0.0001 significant
A-Current	731.75	1	731.75	49.74	0.0001
B-Welding speed	4.91	1	4.91	0.33	0.5793
AB	455.82	1	455.82	30.99	0.0005
A^2	107.73	1	107.73	7.32	0.0268
Residual	117.68	8	14.71		
Lack of Fit	95.46	4	23.86	4.29	0.0935 not significant
Pure Error	22.23	4	5.56		
Cor Total	6150.40	12			
Std. Dev.	3.84		**R-Squared**	0.9809	
Mean	179.34		**Adj. R-Squared**	0.9713	
C.V. %	2.14		**Pred. R-Squared**	0.8912	
PRESS	669.33		**Adeq. Precision**	31.015	

For checking statistically, the adequacy of the model, the normal probability plot (Fig. 13) for the hardness data shows that the residuals generally fall on a straight line, revealing that the errors are normally distributed. Also, from the residuals versus predicted responses plot (Fig. 14) for the hardness results, it's noted that there are no clear patterns or uncommon structure, depicting that the models are accurate. Fig. (15) manifests the predicted hardness versus the actual ones.

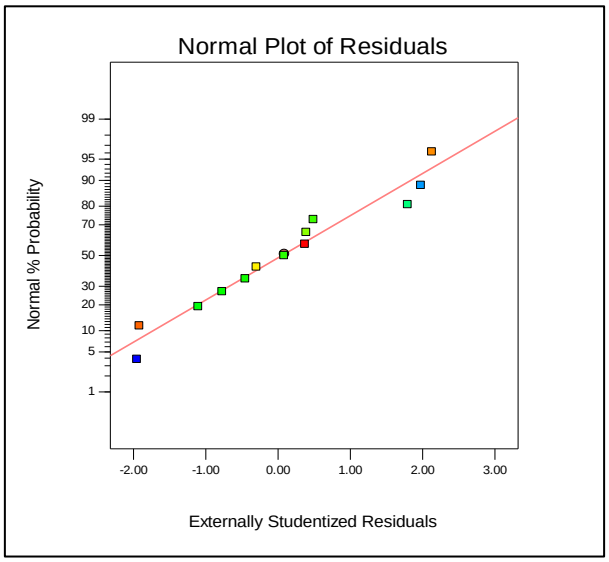

Fig. (13): Normal distribution of hardness data

Fig. (16) demonstrates the 2D contour plot of hardness in terms of welding current and travel speed. Referring to this figure, it can be noticed that the increment in current and travel speed individually causes a higher decrease in the hardness. This means that both current and travel speed have a greater influence on the hardness individually and they proportionate inversely. Regarding the interaction of welding speed and current, this figure also shows that at (325 Amp and 25 cm/min), the combined influence of both factors gives a higher hardness (about 199 HV) than that caused by each one individually.

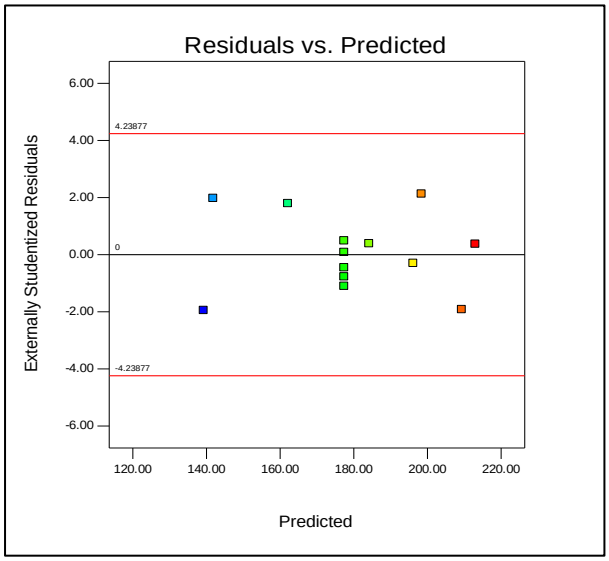

Fig. (14): Residual versus predicted data

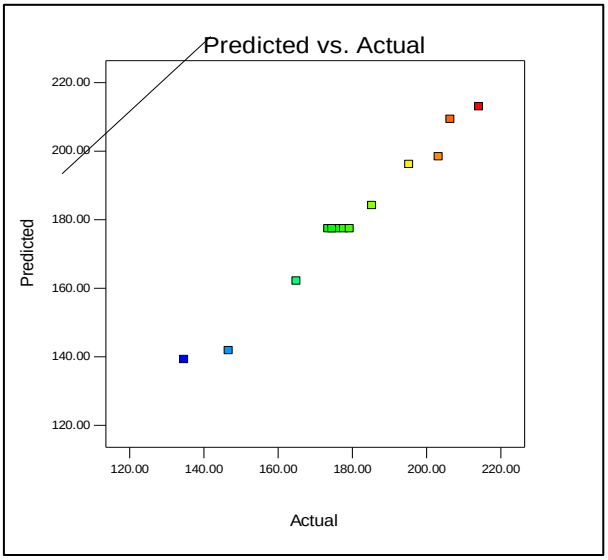

Fig. (15): Predicted versus actual data

Fig. (17) clarifies the 3D graph (surface plot) of hardness as a function of welding speed and current and confirms the observations mentioned in the 2D graph. One can observe that the increment of travel speed and current caused a decrease in the value of hardness at their higher level, whereas at their lower levels, they gave the highest value of hardness. This behavior is thought to be due to the thermal influence on the structure of the welded steel at both lower and higher levels. This is in agreement with ref. [2, 5, 6, 7, 9].

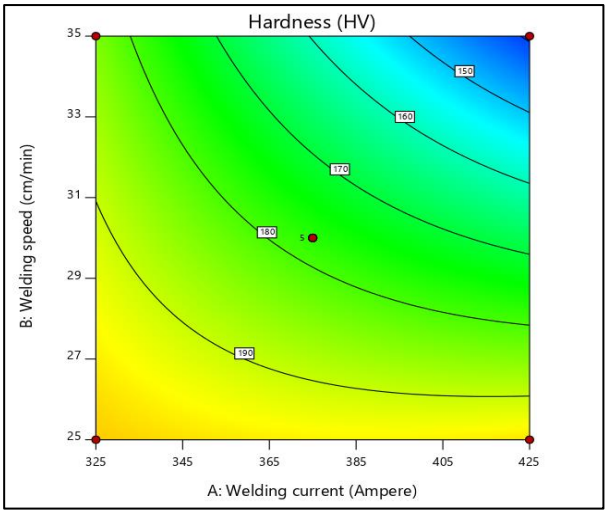

Fig. (16): 2D contour graph of hardness as a function of welding speed and welding current

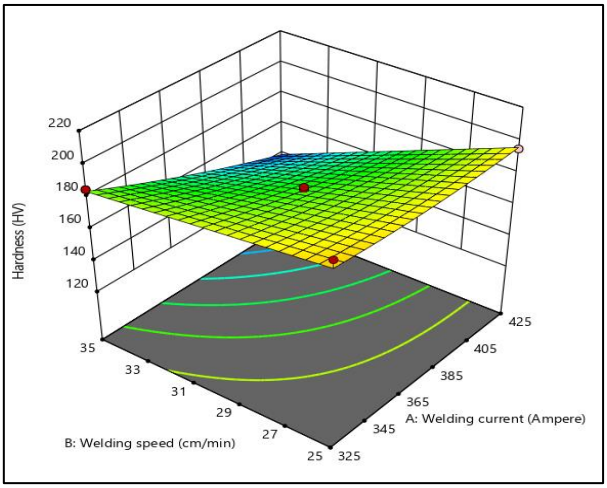

Fig. (17): 3D surface plot of hardness as a function of welding speed and welding current

4. Optimization of Responses

Numerical optimization was employed by the DOE software using the results from Table (5) to obtain the optimum parameters combinations so as to achieve the desired needs, depending on the results from the predicted quadratic models for the mechanical properties as responses (yield stress, bending force and hardness) terms of two input factors (current and travel speed).

The ultimate goal of such optimization was to find the maximum output (response) that at the same time satisfied all the changeable characteristics. Each variable constrains to optimize numerically the yield stress, bending force and hardness were used, and the input factors were selected for their used ranges, while the responses were selected to be the maximum for yield stress and bending force and minimum for hardness. Accordingly, one possible solution satisfied these constrains to find the desired values of the responses (202.659 MPa yield stress, 21.662 KN bending force and 139.232 HV hardness), as shown in Table (9) at the optimum values of welding current (425 Amp) and welding speed (35 cm/min).

Table (9): The optimum values of input factors and responses

Welding current (Amp)	Welding speed (cm/min)	Yield stress (MPa)	Maximum bending force (KN)	Hardness (HV)
425	35	202.659	21.662	139.232

5. Confirmation Tests at the Optimum Conditions

For checking the model's validity, confirmation tests were conducted at the optimum predicted results of the input factors determined in these models in order to measure the yield stress, bending force and hardness. The experimental measurements results are listed together with the predicted data in the Table (10) for purpose of comparison. This table exhibits that the predicted and experimental results possess a good agreement according to the maximum error (1.5%, 1.3% and 3.4%) for yield stress, maximum bending force and hardness, respectively.

Table (10): Results of confirmation tests at the optimum conditions

Welding current (Amp.)	Welding speed (cm/min)	Exp. Yield Stress (MPa)	Pred. Yield Stress (MPa)	Exp. Maximum bending force (KN)	Pred. Maximum bending force (KN)	Exp. Hardness (HV)	Pred. Hardness (HV)
425	35	205.66	202.659	21.95	21.662	134.65	139.232
Error (%)		1.5		1.3		3.4	

6. Joint Efficiency

The efficiency of the joint is a concept that exists in many (API) and (ASME) codes. It's a numerical value that is represented as a percentage, stated as the ratio of a welded, brazed or riveted joint strength to the base material strength. It's also a method for introducing the factors of safety in shells welding for the containment, and it can be written as following [13]:

$$\boldsymbol{Joint\ Efficiency\ (E) = \frac{Yield\ strength\ of\ weld}{Yield\ strength\ of\ base\ material}}$$

Depending on the yield strength values of the material before and after welding, the joint efficiency was 0.534.

7. Conclusions

From the previous results the following concluded points can be obtained:

1- The higher-level of welding speed and the higher level of welding current resulted in the maximum yield stress.

2- The higher level of welding current and the lower level of welding speed gave the maximum value of bending force. However, the welding current was found not influential during welding over the used range of its levels.

3- The increase in both welding speed and current individually results in a higher decrease in the hardness, and both input factors proportionate inversely. Their combined effect at their lower levels gives the highest value of hardness.

4- Depending on the numerical optimization results, the optimum predicted values of the mechanical properties of the steel plate SA-516 Gr. 70 are (202.659 MPa) yield stress, (21.662 KN) maximum bending force and (139.232 HV) hardness at the optimum values of welding current (425 Amp) and welding speed (35 cm/min).

5- According to the outputs of the confirmation tests, a very well agreement was obtained between the predicted and experimental outputs according to the maximum error (1.5%, 1.3% and 3.4%) for yield stress, maximum bending force and hardness, respectively.

Conflict of Interests

There are no conflicts of interest.

References

[1] I. Gowrisankar, A. K. Bhaduri, V. Seetharaman, D. D. N. Verma, and D. R. G. Achar, "Effect of the Number of Passes on the Structure and Properties of Submerged Arc Welds of AISI Type 316L Stainless Steel," *Weld. J.*, pp. 147–154, 1987.

[2] D. M. Viano, N. U. Ahmed, and G. O. Schumann, "Influence of Heat Input and Travel Speed on Microstructure and Mechanical Properties of Double Tandem Submerged Arc High Strength Low Alloy Steel Weldments," *Sci. Technol. Weld. Join.*, vol. 5, no. 1, pp. 26–34, 2000.

[3] A. M. Paniagua-Mercado, V. M. López-Hirata, and M. L. Saucedo Muñoz, "Influence of the Chemical Composition of Flux on the Microstructure and Tensile Properties of Submerged-Arc Welds," *J. Mater. Process. Technol.*, vol. 169, no. 3, pp. 346–351, 2005.

[4] K. Prasad and D. K. Dwivedi, "Microstructure and Tensile Properties of Submerged Arc Welded 1.25Cr-0.5Mo Steel Joints," *Mater. Manuf. Process.*, vol. 23, no. 5, pp. 463–468, 2008.

[5] A. Harish, S. Kulwant, and S. Sanjay, "Cooling Rate Effect on Microhardness for SAW Welded Mild Steel Plate," *Int. J. Theor. Appl. Res. Mech. Eng.*, vol. 2, no. 2, pp. 71–77, 2013.

[6] R. Kumar, H. K Arya, and S. RK, "Experimental Determination of Cooling Rate and its Effect on Microhardness in Submerged Arc Welding of Mild Steel Plate (Grade c-25 as per IS 1570)," *Mater. Sci. Eng.*, vol. 03, no. 02, 2014.

[7] N. Singh, Karun, S. Kumar, and D. Singh, "Investigating the Effect of Saw Parameters on Hardness of Weld Metal," *Int. J. Adv. Ind. Eng.*, vol. 3, no. 2, pp. 68–74, 2015.

[8] S. A. Amin, S. H. Bakhy, and F. A. Abdullah, "Study the Effect of Welding Parameters on the Residual Stresses Induced by Submerged Arc Welding process," *Al-Nahrain J. Eng. Sci.*, vol. 20, no. 4, pp. 945–951, 2017.

[9] S. H. Bakhy, S. A. Amin, and F. A. Abdullah, "Influence of SAW Welding Parameters on Microhardness of Steel A516-Gr60," *Eng. Technol. J.*, vol. 36, no. 10, pp. 1039–1047, 2018.

[10] ASME, *ASME, BPVC, Sec.II: Materials, Part A: Ferrous Material Specificatios (SA-451 to End)*. The American Society of Mechanical Engineers, 2015.

[11] ASME, *ASME, BPVC, Sec. II: Materials, Part C: Specifications for Welding Rods, Electrods and Filler Metals*. The American Society of Mechanical Engineers, 2015.

[12] Askanyak company, "Eczacıbaşı - Lincoln Electric ASKAYNAK ® Products." www.askanyak.com.tr.

[13] ASME, *ASME, BPVC, Section VIII, Division 1: Rules for Construction of Pressure Vessels*. 2015.

دراسة الخواص الميكانيكية للصلب الكربوني (SA-516 Gr. 70) الملحوم بالقوس المغمور بأستخدام تصميم وصلة لحام مربعة الشكل

مهند يوسف حنا سمير علي امين عبد العزيز سعود خضر

قسم الهندسة الميكانيكية، الجامعة التكنولوجية، بغداد، العراق

abdulaziz.saud87@gmail.com alrabiee2002@yahoo.com mohannad_hanna@yahoo.com

الخلاصة

ان لحام القوس المغمور هو لحام انصهاري من حيث النوع ويعتبر أحد عمليات اللحام المهمة لقابلياته الذاتية من حيث سرعة اللحام، معدل الترسيب العالي، ولحام الواح ذات سمك كبير بسبب خاصية النفاذية العميقة وفوائد متعددة اخرى. تهدف هذه الدراسة الى التحقق من تأثير عوامل اللحام (تيار اللحام وسرعة اللحام) بالإضافة الى تصميم وصلة اللحام على الخواص الميكانيكية (اجهاد الخضوع، قوة الحني على وجه الملحومة وصلادة مادة منطقة اللحام). اجريت التجارب باستخدام برنامج تصميم التجارب (DOE) وتقنية طريقة الاستجابة السطحية (RSM). انجزت التجارب بلحام (26) قطعة من لوح سبيكة الصلب نوع (ASME SA-516 Gr. 70) بأبعاد (300 ملم x 150 ملم x 10 ملم) لتصنيع (13) عينة ملحومة اعتمادا على مصفوفة التصميم الناتجة من برنامج تصميم التجارب. اظهرت النتائج بأن العوامل المثلى لعملية اللحام لأقصى اجهاد خضوع، أقصى قوة حني وأدنى صلادة هي (202.659 ميكا باسكال، 21.662 كيلو نيوتن، و 139.232صلادة فيكرية) على التوالي عند تيار لحام (425 أمبير) وسرعة لحام (35 سم/ دقيقة) مع بقاء فولتية القوس ثابت عند (37 فولت). أخيرا، وجد ان النتائج المتنبأة والعملية لاجهاد الخضوع وقوة الحني والصلادة في توافق جيد مع اقصى مقدار خطأ (1.5%، 1.3% و3.4%) على التوالي.

الكلمات الدالة: عوامل اللحام، لحام القوس المغمور، الخواص الميكانيكية، تصميم التجارب، طريقة الاستجابة السطحية